# Probabilistic Analysis of In Situ Soil Water Characteristic Curve Using Kernel Density Estimation

Md. Jobair Bin Alam, Ph.D., P.E., M.ASCE<sup>1</sup>; Maalvika Aggarwal, S.M.ASCE<sup>2</sup>; and Naima Rahman, Ph.D., M.ASCE<sup>3</sup>

<sup>1</sup>Assistant Professor, Dept. of Civil and Environmental Engineering, Prairie View A&M Univ., TX. Email: mdalam@pvamu.edu

<sup>2</sup>Undergraduate Research Assistant, Dept. of Civil and Environmental Engineering, Prairie View A&M Univ., TX. Email: maggarwal@pvamu.edu

<sup>3</sup>Project Professional, SCS Engineers, Houston, TX. Email: nrahman@scsengineers.com

### **ABSTRACT**

Soil water characteristic curve (SWCC) which describes the relationship between water content and matric suction is important to analyzing unsaturated soil behavior. Because of the degree of uncertainty in field conditions due to climatic variability and soil heterogeneities, it becomes necessary to probabilistically characterize the SWCC. A satisfactory probabilistic characterization of field-based SWCCs requires a substantial data pair of water content and suction and their distribution characteristics. In this study, the kernel density estimate (KDE) approach was applied to water content and suction data measured from field-installed co-located sensors of a compacted clay bed to (1) determine the modality of water content and suction distribution and their constitutive relationship at variable weather conditions and (2) demonstrate the importance of probabilistic analysis of SWCC. The Gaussian function was used in the KDE analysis. A moisture sensor and soil water potential sensor were juxtaposed at 0.3 m depth of the 3 m × 3 m compacted clay bed to collect the water content and suction data and determine their distribution under the field condition. The density plots of both water content and suction at 0.3 m depth exhibited multimodal distribution due to the uneven distribution of climatic events. The KDE reasonably identified the air entry value, saturated moisture content, and residual moisture content in the field conditions, which were validated with field-based SWCC plots. The study showed that probabilistic analysis better interprets the realistic scenarios of field unsaturated soil behavior.

## INTRODUCTION

Soil-water characteristic curve (SWCC) is the constitutive relationship between soil suction  $(\psi)$  and water content  $(\theta)$ . This constitutive relationship between  $\theta$  and  $\psi$  is important to analyzing unsaturated soil behavior (unsaturated shear strength and unsaturated hydraulic conductivity) of geotechnical engineering infrastructures such as unsaturated slopes, pavement subgrades, landfill covers, etc. SWCC is developed through many laboratory techniques where the different scatter points of  $\theta$  and the correspondent  $\psi$  are measured, and the scattered points are fitted through a function such as van Genuchten (1980), which represents the shape of the SWCC. However, laboratory-based SWCC determination has certain disadvantages such as being time-consuming (Lu and Likos, 2004), limitations of equipment to cover the entire suction range of soil, and alteration of the natural physical properties of soil during sampling. Most importantly, SWCC construction in the laboratory is conducted in controlled environmental

conditions (Basile et al. 2003; Zhang et al. 2017), which is not representative of the variable natural field conditions. In addition, SWCC is not unique for a particular soil, which was considered a unique characteristic for a particular soil type. It is now well-established that one specific soil may have different SWCC curves due to various sources of uncertainties contributed by equipment choice of SWCC measurement, the capacity of the SWCC measuring range of the equipment, the initial density of the soil sample, hysteresis phenomenon, temperature, and chemical composition of pore water, etc. (Prakash et al. 2020). The uncertainties may even be extreme in field conditions due to variable climatic conditions, wet-dry cycle, root growth, crack formation, etc. Therefore, understanding the field variation of  $\theta$  as a function of  $\psi$  seems more important to estimating site-specific unsaturated soil properties to better represent the realistic hydrological features of the soil to increase the reliability in the analysis and design of earth infrastructures (Fredlund et al. 2012).

The probabilistic approach has been proven to be a useful tool to account for the uncertainties arising out of the field conditions that affect the shape of the SWCC. Most of the previous studies have used probability theory in parameterizing the SWCC. For example, the joint distribution of van Genuchten SWCC parameters  $(\alpha, m, n)$  proposed by Carsel et al. (1988), the joint lognormal translational model for constructing the joint density of van Genuchten parameters (Phoon et al. 2010), use of the Bayesian approach of the probability distribution of van Genuchten SWCC parameters (Chiu et al. 2012), etc. are some of the approaches. However, most of the approaches mentioned above have used a certain database containing limited data such as the UNSODA (Nemes et al. 2001) of SWCC for a particular soil texture, which is certainly very useful for understanding the nature of the variability of the SWCC parameters. Nonetheless, it is still not adequate to understand the field behavior since it doesn't explain the field dynamics because the in-situ change of  $\theta$  as a function of  $\psi$  was not captured in any database. Increasing the reliability of the estimated SWCC through probabilistic analyses requires a large amount of test data obtained from different soil samples for a given type of soil (e.g., Phoon et al. 2010). However, it is very unlikely to have site-specific sufficient availability of data. Field instrumentation-based measurement of  $\theta$  and  $\psi$  may provide an adequate dataset to address this concern of limited field SWCC data. In addition, field instrumentation provides continuous measurement of  $\theta$  and  $\psi$  at any point of interest, and most importantly it captures the field dynamics. Though point measurement of SWCC through instrumentation may not be representative of a sizeable earth infrastructure and the overall field conditions, probabilistic analyses of the point measurement of the constitutive parameters:  $\theta$  and  $\psi$  may provide useful insight into the in-situ unsaturated soil behavior.

For any statistical and probabilistic analyses, it is pivotal to understand the distribution of the variables. The distribution of the data identifies any significant asymmetries, discontinuity of data, and multimodal peaks. Density estimate or probability density function (PDF) is one of the common techniques in characterizing data distribution. The in-situ changes in  $\theta$  and  $\psi$  during field meteorological events may take any random unimodal to multimodal distributions depending on the intensity and frequency of the meteorological events, and other factors. Hence, characterizing  $\theta$  and  $\psi$  distribution under field conditions should be the first step to understanding the dynamics of field SWCC. Therefore, a smooth density estimate of  $\theta$  and  $\psi$  is necessary. This study used the nonparametric method: Kernel Density Estimate (KDE) to characterize the  $\theta$  and  $\psi$  distribution, measured at a shallow depth of a compacted clay bed (3 m × 3 m), and the key features of the van Genuchten SWCC model were estimated probabilistically. The  $\theta$  and  $\psi$  were measured using moisture sensors and tensiometers, which

were installed at collocated depth (0.3 m). The KDE is commonly used in a more general statistical context to obtain smooth estimates of probability densities from sample observations (Silverman, 1986). Such a PDF estimate appears to reflect a continuous variable's true PDF more accurately.

# KERNEL DENSITY ESTIMATE (KDE)

The KDE signifies a weighted moving average of the frequency distribution of the data. It requires the use of a kernel function (K(x)) such as Gaussian kernel, triangular kernel (Burt and Barber 1996), quartic kernel (Bailey and Gatrell 1995), and Epanechnikov's kernel (Epanechnikov 1969). This study used the Gaussian kernel function (Equation 1). The KDE of a probability density function (PDF) of a variable x is defined by Equation (2) as presented below.

$$K(x) = \frac{1}{\sqrt{2\pi}} e^{(-\frac{x^2}{2})}$$
 (1)

$$f_h(x) = \frac{1}{nh} \sum_{i=1}^{n} K\left(\frac{x - X_i}{h}\right)$$
 (2)

where h is the bandwidth and n is the sampling size, two main parameters affecting the KDE, and  $X_i$  is the observed data points. A large sample can give a better resolution of the KDE. In the present analysis, the sample size was more than adequate, with almost 36000 data. In this study, to select the ideal bandwidth h, we used the program R-implemented Sheather and Jones (1991) method because of its broader use and being well-regarded for bandwidth optimization in KDE with sufficient theoretical justification (Sheather 2004).

## MATERIALS AND METHOD

The study was conducted at the research and demonstration farm (RDF) of Prairie View A&M University in Waller County. The compacted clay bed was constructed with a dimension of 3 m × 3 m and 1.22 m deep. Construction activities are presented in Figure 1.

The existing subgrade was excavated up to 1.2 m (Figure 1a), and the bottom of the pit was sloped at 2% to allow water to flow toward the sloping end under gravitational action. The subgrade bottom and side wall were overlain by a 6-mil impermeable plastic sheet. After the placement of the plastic sheet, the bed was backfilled with the excavated fine-grained soil (Figure 1b) and compacted to 95% of optimum moisture content. During the excavation period, soil samples were collected from the test bed. The collected samples were subjected to laboratory characterization according to the ASTM standards (ASTM D 422-63, ASTM D 4318, ASTM D 2487, ASTM D 698). Based on the laboratory characterization of the collected samples, the fine fractions of the samples were estimated to be more than 70%. The soil's liquid limit and plasticity index were found to be almost 52% and 27%, respectively. According to the Unified Soil Classification System (USCS), the soil was classified as Fat Clay with Sand (CH). After the backfilling, a moisture sensor, and soil water potential sensor were installed and collocated at 0.3 m depth to closely monitor field SWCC (Figure 1c). The schematic of sensor installation is

presented in Figure 1(e). The sensors used in this study are TEROS 21: soil water potential sensors, and TEROS 11: moisture and temperature sensors manufactured by Meter Group. This study investigated the  $\theta$  and  $\psi$  data distribution and field SWCC obtained during the 6-month monitoring of the sensors. The sensors installed at the test bed were connected to an automatic data logging system, and both were adjusted to collect data in equivalent time intervals. The sensors were calibrated following the user's manual before field installation. A weather station was also installed (Figure 1d) to evaluate the field SWCCs in response to climatic variations at the site.

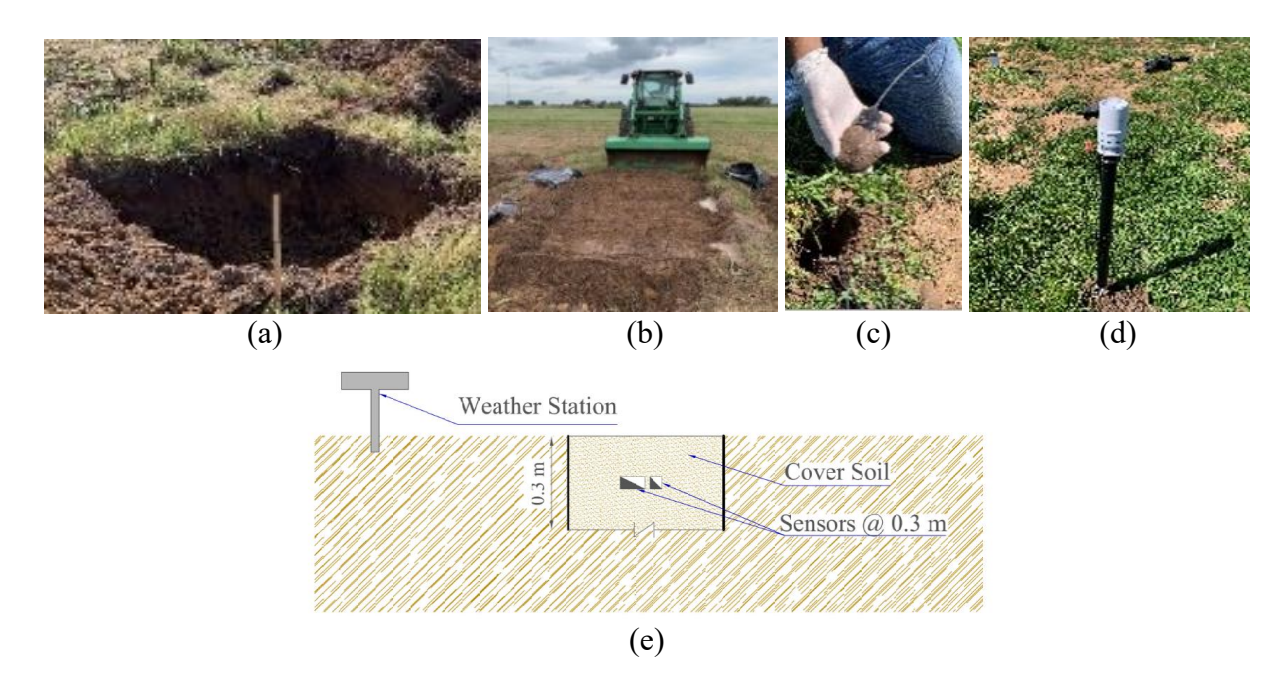


Figure 1. (a) Excavation of the test pits (b) soil backfilling after a 6-mil plastic sheet placement (c) drilling holes and sensor installation (d) installed weather station (e) instrumentation schematic

#### RESULTS AND DISCUSSION

# Variation in Soil Moisture and Suction Under Field Conditions

The changes in  $\theta$  and corresponding variations of  $\psi$  under the fluctuating field conditions are presented in Figure 2(a). The site precipitation data are presented in Figure 2(b). It is to be noted that both the moisture sensor and soil water potential sensor and the weather station were adjusted to record data at identical time intervals (every 5 minutes). The exactness of the installed sensors at the site in capturing the field hydrological behavior under the climatic variations was adequate as observed in Figure 2(a), and when correlating between Figure 2(a) and 2(b). It is observed that both the  $\theta$  and  $\psi$  abruptly changed during the wetting of the soil (increase in  $\theta$  and decrease in  $\psi$ ) when precipitation events of more than 3 mm (Figure 2a) were recorded, indicating the soil at shallow depths of the clay cover was highly responsive to climatic variability. However, the drying of soil was significantly slower relative to the wetting. During every drying process (5 dryings were recorded during the monitoring period), the rate of drying was different but comparable depending on the ambient temperature and other site variables.

Apparently, Figure 2(a) indicates the saturated volumetric moisture content ( $\theta_s$ ) to be 0.36 m<sup>3</sup>/m<sup>3</sup>. However, one interesting point was observed in Figure 2(a): at the inception of every drying of the soil, the  $\theta$  was approximately near 0.30 m<sup>3</sup>/m<sup>3</sup>. It implies that at the field conditions of the soil, the largest pores started to desaturate at approximately 0.30 m<sup>3</sup>/m<sup>3</sup>, which is associated with the air entry value (AEV). The  $\psi$  at which the soil starts to desaturate (air begins to enter the soil's largest voids) is called the AEV or air entry suction. In Figure 2(a), deterministically, locating the AEV appeared difficult. During field monitoring (approximate observation between 20000 to 30000 in Figure 2a), when no precipitation was recorded (Figure 2b) and high temperature prevailed at the site, the  $\psi$  precipitously rose to almost 2020 kPa and remained constant until the next precipitation events. The decreasing rate of  $\theta$  during that time was significantly slower, indicative of  $\theta$  reaching the residual moisture ( $\theta_r$ ) condition (almost 0.12 m<sup>3</sup>/m<sup>3</sup> according to Figure 2a). Based on the variation of  $\theta$  and  $\psi$  under the field climatic conditions as presented in Figure 2(a), the field SWCC features were depicted, however, the SWCC features couldn't be comprehensively identified.

In addition to illustrating the field variations of the  $\theta$  and  $\psi$ , fundamental statistical characteristics of the monitored data were evaluated. Descriptive statistics of the monitored  $\theta$  and  $\psi$  are listed in Table 1. The central tendency of both  $\theta$  and  $\psi$  indicates a high degree of dispersion, especially for  $\psi$ , which is quite comprehensible. The minimum  $\psi$  was recorded at 0.4 kPa during the field monitoring. It is to be noted that the suction readings in the soil water potential sensor used in this study didn't exhibit 0 kPa suction after any precipitation events. Hence, it is rational to assume the 0.4 kPa suction represents the saturated condition of the soil. The mode of  $\psi$  was estimated to be 0.6 kPa, which is very close to the field's minimum  $\psi$  (0.4 kPa) value. Therefore, the occurrences of soil being at saturated conditions were higher than any other soil status. The mode of  $\theta$  was 0.281 m³/m³. Ideally, to be in congruence with  $\psi$ , the mode of  $\theta$  should also represent the saturated condition of the soil. However, analyzing the  $\theta$  variability where the maximum  $\theta$  value was 0.366 m³/m³, deterministically, it is difficult to ascertain this. Hence, a probabilistic approach may be useful.

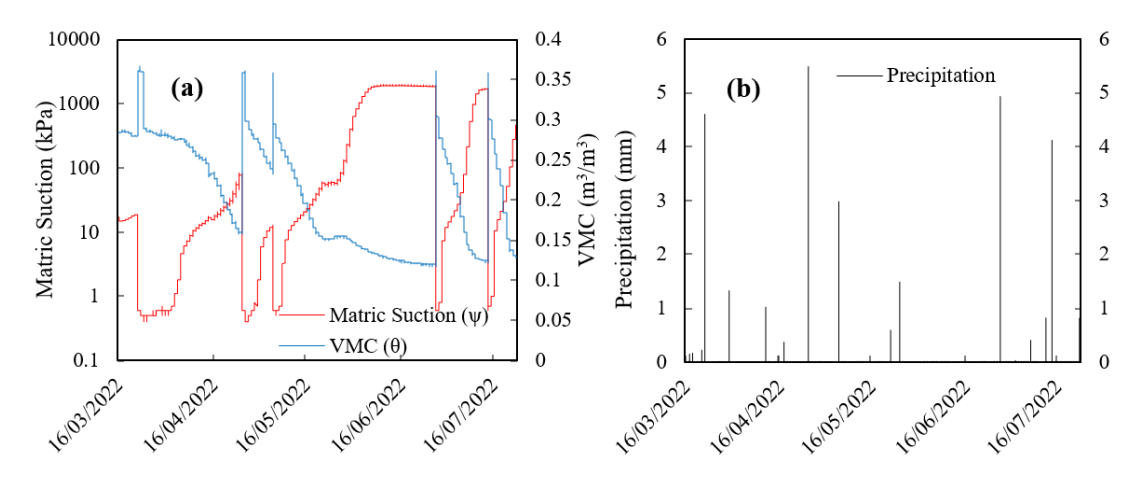


Figure 2. (a) Variation in  $\theta$  and  $\psi$  (b) precipitation

# **KDE-Based Modality Analyses of Field-Monitored Soil Moisture and Suction**

The KDE method was applied to the field-monitored  $\theta$  and  $\psi$  data. The major feature of the KDE is presented in Table 2. The optimum bandwidth (h) for  $\psi$  and  $\theta$  was estimated to be 54.62

and 0.0075, respectively, depending on the variabilities and data range of  $\psi$  and  $\theta$ . In an ideal condition, the change in  $\theta$  would make an immediate associated equivalent change in  $\psi$  value. In other words, the change in  $\theta$  and  $\psi$  or the SWCC would be coherently instantaneous. Hence it is quite reasonable to assume that in the distribution of  $\theta$  and  $\psi$ , the densities of  $\theta$  and  $\psi$  at their concerned values must be coherent. For example, in a  $\theta$  and  $\psi$  distribution, if the density of  $\psi$  appears to be an arbitrary number " $\beta$ " at a very low suction (saturated condition or AEV), then it is expected that  $\beta$  equivalent density of  $\theta$  would represent the saturated water content ( $\theta_s$ ). Or if the density of  $\psi$  is " $\beta$ " at a high suction (dry condition), then  $\beta$  equivalent density of  $\theta$  should represent the residual water content ( $\theta_r$ ). The maximum densities of  $\psi$  (0.0048) at 15.678 kPa and  $\theta$  (10.32) at 0.281 m<sup>3</sup>/m<sup>3</sup> differ significantly, indicating the changes in  $\theta$  and  $\psi$  or SWCC may not necessarily be simultaneous and well-proportioned in the varying field conditions.

**Table 1. Descriptive Statistics** 

<b>Descriptive Statistics</b>	Matric Suction (kPa)	$VMC (m^3/m^3)$
Mean	464.07	0.208
Median	19.7	0.216
Mode	0.60	0.281
Standard Deviation	758.272	0.068
Kurtosis	-0.337	-1.240
Skewness	1.238	0.158
Minimum	0.40	0.117
Maximum	2019.7	0.366

Table 2. The major feature of KDE

KDE Features	Matric Suction	VMC
Bandwidth (h)	54.616	0.0075
Maximum Density	0.0048	10.319
Corresponding Values	15.678 (kPa)	$0.281  (m^3/m^3)$

The KDE-estimated PDFs of  $\theta$  and  $\psi$  are presented in Figure 3. The PDF of  $\psi$  has two distinct densities (at 0.00483 and 0.00101) apparently implying a bimodality of  $\psi$  distribution in the field. However, in actuality, the  $\psi$  distribution is multimodal where most of the peaks (densities) of the data distribution are significantly low. Whereas the  $\theta$  has multiple noticeable densities, with three distinct densities at three different locations: 10.10 at 0.126 m³/m³, 10.32 at 0.281 m³/m³, and 1.44 at 0.36 m³/m³. These distinct densities of  $\theta$  and  $\psi$  may have a major magnitude in the field of SWCC characterization.

Here,  $0.126 \text{ m}^3/\text{m}^3$  possibly represents the soil's residual moisture content. It is to be noted that, the unsaturated characterization of the soil in the laboratory revealed the soil's  $\theta_r$  and  $\theta_s$  in the range between 0.09 to 0.13 m³/m³, and 0.39 to 0.42 m³/m³, respectively. The moisture content of 0.36 m³/m³ in the PDF plot (Figure 3) has a relatively lower density though it has a distinguishable peak. It may be reasonable to assume that 0.36 m³/m³ is the saturated volumetric moisture content, however, the lower density of 0.36 m³/m³ makes the inference debatable since the maximum density of the  $\theta$  (10.32) was obtained at 0.281 m³/m³ as shown in Figure 3. Though comparing the laboratory test results, 0.281 m³/m³ doesn't seem to be the saturated

volumetric moisture content, however, its high density (maximum) in the PDF and potential alteration in the soil structural orientation due to natural processes (e.g., wetting-drying cycle) may reduce the saturated volumetric moisture content under the field conditions. Previous research indicated that different degrees of saturation can be obtained for the same soil at the same suction due to the variation in dry density, hysteresis, different test methodologies, variability in test procedures, and operator error (Zapata 1999). In the field conditions, the probability of this phenomenon is even higher because of the wetting-drying, freezing-thawing, development of macro pores, pedogenesis, soil desiccation, and other forms of uncertainties.

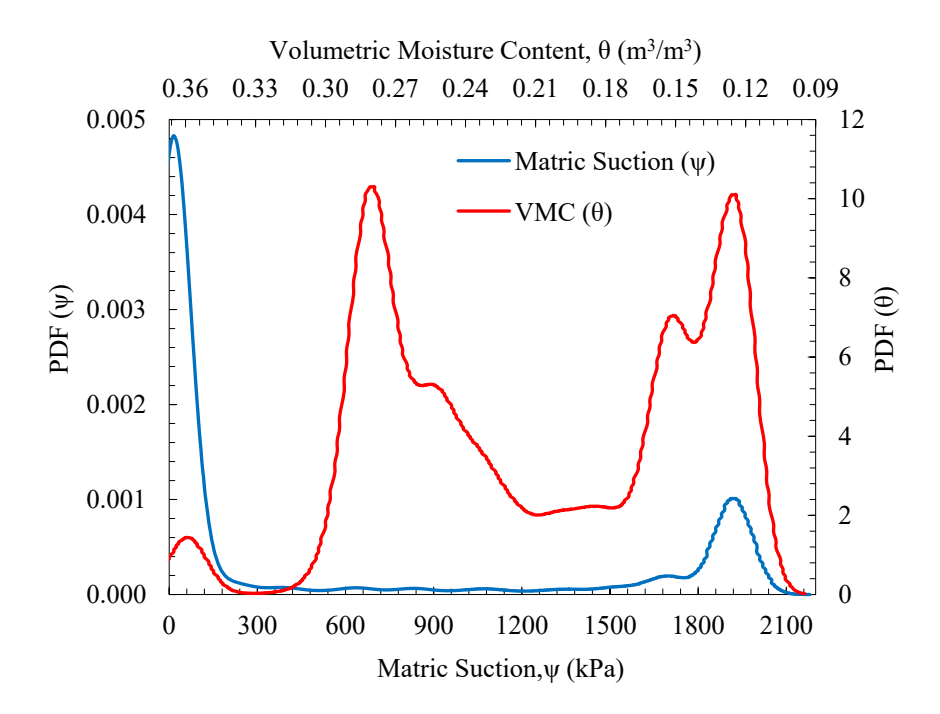


Figure 3. KDE-based PDF of  $\theta$  and  $\psi$ 

The two distinct  $\psi$  values identified in Figure 3 are 15.7 kPa (PDF=0.00483), and 1920 kPa (PDF=0.00101). The 1920 kPa suction is the most probable suction attained by the soil in the field at the dry condition and can be coupled with the most probable residual soil moisture ( $\theta_r$  = 0.126 m³/m³ at PDF=10.10). This can further be explained from the field-based plot of SWCC. Field SWCC was constructed by coupling simultaneous field measurements of  $\theta$  and  $\psi$ . It is to be noted that the laboratory-measured SWCC was not included here for comparison, rather it was attempted to observe the field behavior. Field-constructed SWCCs were mathematically described by using van Genucthen's closed-loop equation (van Genuchten, 1980) as presented in Equation 3. It is to be noted that the van Genuchten model was generated to represent the overall shape of the field SWCC. Individual paths (sorption or desorption) were not considered.

$$\theta = \theta_{\rm r} + \frac{\theta_{\rm s} - \theta_{\rm r}}{[1 + (\alpha \Psi)^{\rm n}]^{\rm m}} \tag{3}$$

where  $\theta$  is the water content corresponding to matric suction  $\psi$ ;  $\theta_s$  is the volumetric water content at the saturated condition;  $\theta_r$  is the residual volumetric water content; and  $\alpha$ , n, and m are van

Genuchten's SWCC curve fitting parameters. Field-coupled data points and the van Genuchten model SWCC are presented in Figure 4. The field observations show multiple paths (drying) indicating hysteresis and retaining a sigmoidal shape with two obvious asymmetries. These paths are also referred to as the scanning curves (transition between wetting and drying). The wetting curves didn't appreciably appear in the field SWCC plot because of the significantly faster response time of the changes in  $\theta$  and  $\psi$  during field imbibition (precipitation infiltration). Investigating the shape of the field SWCC (Figure 4), it can be attributed that there are three distinct stages of SWCC incurred from the field conditions - (1) boundary effect stage, (2) transition stage, and (3) residual stage. The boundary effect stage represents the soil's saturated conditions until the AEV. The AEV appeared to be around 13 kPa in Figure 4. In the transition stage, the soil starts the desorption process until it reaches the residual stage. The residual stage signifies the zone of the SWCC where there are no appreciable changes in  $\theta$  with  $\psi$ , and it depicts the  $\theta$ r. In Figure 4, the minimum  $\theta$  ( $\theta$ r) beyond which there is no significant variation in  $\theta$  with  $\psi$  is around 0.13 to 0.14 m<sup>3</sup>/m<sup>3</sup>.

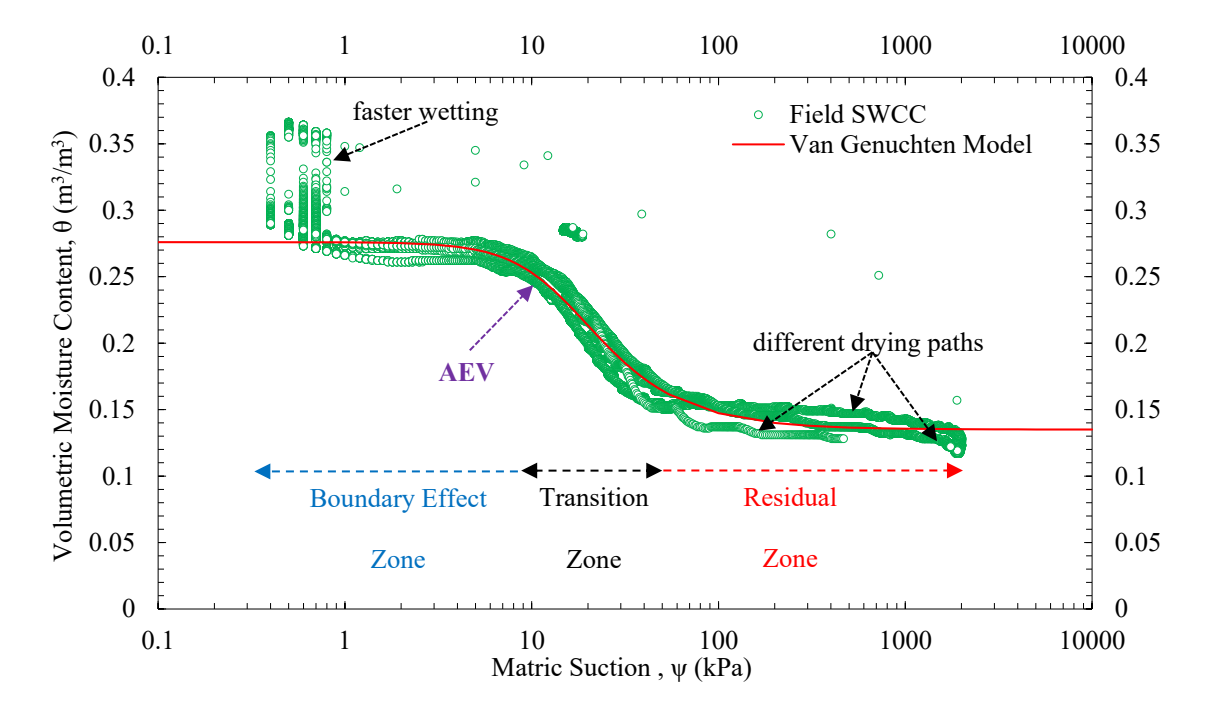


Figure 4. Field soil water characteristic curve

The van Genuchten model parameters are listed in Table 3. The  $\theta_s$  and  $\theta_r$  were estimated to be 0.281 and 0.13 m<sup>3</sup>/m<sup>3</sup>, respectively. The shape parameter  $\alpha$  appeared to be 0.065 which is related to the inverse of the AEV (15.38 kPa). Comparing the distinguishable densities of  $\psi$  distribution in Figure 3, the 15.7 kPa with maximum density (PDF=0.00483) almost certainly represents the most probable AEV in the field conditions. It can be explained that after any wetting process, the  $\psi$  data (large quantity) distribution was constricted in the boundary effect zone around the AEV until the required energy for the soil to enter the transition stage was achieved. In the transition stage, SWCC changes rapidly as indicated by the higher slope parameter of the van Genuchten curve (n=2.301). Accordingly, the data distribution or the densities within the transition stage is very low. In the residual zone, both  $\theta$  and  $\psi$  have discernible high densities ( $\theta$  ( $\theta_r$ ) = 0.126 m<sup>3</sup>/m<sup>3</sup> at PDF=10.10, and  $\psi$  =1920 kPa at

PDF=0.00101). The PDF in Figure 3 also has a distinct density at 0.366 m<sup>3</sup>/m<sup>3</sup> (PDF=1.44). Since the PDF of 0.366 m<sup>3</sup>/m<sup>3</sup> is lower than the maximum density at 0.281 m<sup>3</sup>/m<sup>3</sup> (PDF=10.32), it is reasonably attributable to the fact of the faster wetting of the soil due to immediate response of precipitation as indicated by the abrupt rises in  $\theta$  in Figure 2(a). Based on the data distribution of  $\theta$  and  $\psi$ , and the volume of data analyzed in this study, we anticipate that more precipitation events (consider including a large volume of  $\theta$  and  $\psi$  monitored for a few years with significant climatic events) would have increased the PDF at 0.36 m<sup>3</sup>/m<sup>3</sup>.

Table 3. Model parameter of van Genuchten function

SWCC Element	Value
Saturated volumetric water content $(\theta_s)$	0.281
Residual volumetric water content $(\theta_r)$	0.130
van Genuchten Model Parameter	Value
$\alpha$	0.065
AEV	$15.38 \rightarrow (1/\alpha) = (1/0.065) = 15.38 \text{ (kPa)}$
n	2.301

### PRACTICAL SIGNIFICANCE

Under the field condition, it is practically impossible to be deterministic in the characterization of SWCC. In addition, various uncertainties incurring in the field conditions that affect the SWCC are extremely difficult to appreciate. For practical engineering practice in geotechnical engineering, especially in designing and failure analysis of earth embankments, pavement subgrade, landfill covers, etc., the key unsaturated soil properties such as AEV, residual, and saturated moisture contents are extremely important. Therefore, precise estimation of these parameters is crucial. However, since environmentally-controlled laboratory-measured SWCCs are not representative of field application in most cases and deterministically characterizing the SWCCs in the field is infeasible, hence, probabilistically describing the field SWCCs is practically the best choice to identify the most probable unsaturated soil parameters. In this study, a simple but efficient probabilistic approach, KDE analyses were conducted using field monitoring data to investigate the distribution of  $\theta$  and  $\psi$  and characterize the SWCC features. Investigating the densities of  $\theta$  and  $\psi$ , it was observed that the discernible densities may detect a few of the required features of SWCC, and the  $\theta$  and  $\psi$  associated with these densities represented the required most probable SWCC elements (e.g., AEV,  $\theta_r$ , etc.) after analyzing the shape of the field-coupled SWCC. Though the density analyses of  $\theta$  and  $\psi$  of this study are sitespecific, the bivariate analyses using the KDE provided a useful tool for characterizing the unsaturated soil parameters and potentially can be used as a preliminary predictive tool of field unsaturated soil behavior for South Texas. For any project of special significance such as earth infrastructures constituting problematic soil or expansive soil in humid climate regions, that requires realistic estimates of the unsaturated soil parameters, a site instrumented with necessary sensors and analyses with a few years' monitoring data using the KDE may establish a representative foundation of projected SWCC behavior for that region.

#### CONCLUSION

Soil moisture content ( $\theta$ ) and matric suction ( $\psi$ ) distribution characteristics evaluated from co-located field-installed sensors of a compacted clay bed have been presented in this study. The PDFs of the measured  $\theta$  and  $\psi$  were analyzed using the Kernel Density Estimate (KDE) which provides a smooth optimization of data frequency. The data analysis conducted in the statistical environment demonstrated that the higher and distinguishable densities in the KDE plot technically indicated some probable key features of SWCC such as the air entry value, and saturated and residual volumetric moisture contents. However, it was observed that there were significant dissonances in the distinct densities of  $\theta$  and its corresponding  $\psi$ . These discordances in the PDFs at the equivalent  $\theta$  and  $\psi$  could be due to various reasons in the field, however, practically impossible to appreciably identify. Investigating the sigmoidal-shaped field SWCC and van Genuchten model parameters, the AEV in the field conditions appeared to be almost 15.38 kPa, which was detected in the KDE-generated PDF (15.7 kPa) at a density of almost 0.00483. The ascription of this phenomenon was understood after investigating the data distribution where a large percentage of the monitored data pairs ( $\theta$  and  $\psi$ ) were around the AEV. The saturated and residual volumetric moisture contents from the discernible peaks of the PDFs were identified to be 0.281 and 0.126 m<sup>3</sup>/m<sup>3</sup>, respectively. These  $\theta_s$  and  $\theta_r$  values from the plot of the field SWCC were also in agreement with the evaluation from the PDFs. Overall, the KDE-based density analyses to characterize the field unsaturated soil behavior was positive, however, increasing the robustness of the KDE application in characterizing the field SWCCs will require long-term monitoring data, and at different climatic regions (e.g., humid, arid, semiarid, etc.), and with different soils (e.g., CH, CL, SC, ML, etc.).

## **ACKNOWLEDGEMENT**

The authors gratefully acknowledge the funding provided for this research by the National Science Foundation (NSF), grant number #2101081. The authors are also grateful to *Watershed Geo* for providing technical guidance and support during the engineered turf installation.

### REFERENCES

- Alam, M. J. B., and Hossain, M. S. 2019. Evaluation of post-construction changes in soil hydraulic properties through field instrumentation and in situ testing. In *Geo-Congress 2019: Geotechnical Materials, Modeling, and Testing* (pp. 722-732). Reston, VA: American Society of Civil Engineers.
- Alam, M. J. B., Ahmed, A., Hossain, M. S., and Rahman, N. 2021. Estimation of percolation of water balance cover using field-scale unsaturated soil parameter. In *MATEC Web of Conferences* (Vol. 337, p. 04005). EDP Sciences.
- Nemes, A. D., Schaap, M., Leij, F., and Wösten, J. 2001. Description of the unsaturated soil hydraulic database UNSODA version 2.0, *J. Hydrol.* 251 (3-4), 151–162.
- Prakash, A., Hazra, B., and Sekharan, S. 2000. Probabilistic analysis of soil-water characteristic curve of bentonite: multivariate copula approach, *Int. J. Geomech.* 20 (2) 04019150.
- Basile, A., Ciollaro, G., and Coppola, A. 2003. Hysteresis in soil water characteristics as a key to interpreting comparison of laboratory and field measured hydraulic properties. *Water Resour. Res.* 39 (12), 1–12.

- Burt, J. E., and Barber, G. M. 1996. *Elementary Statistics for Geographers*, 2nd edn. The Guilford Press, New York.
- Bailey, T. C., and Gatrell, A. C. 1995. *Interactive Spatial Data Analysis*. Longman Higher Education, Harlow.
- Chiu, C., Yan, W., and Yuen, K.-V. 2012. Reliability analysis of soil—water characteristics curve and its application to slope stability analysis, *Eng. Geol.* 135, 83–91.
- Epanechnikov, V. A. 1969. Nonparametric Estimation of a Multivariate Probability Density. *Theory of Probability and Its Applications* 14, 153–158.
- Fredlund, D. G., Rahardjo, H., and Fredlund, M. D. 2012. *Unsaturated Soil Mechanics in Engineering Practice*. John Wiley & Sons, Inc., Hoboken, New Jersey.
- Lu, N., and Likos, W. J. 2004. *Unsaturated Soil Mechanics*. John Wiley & Sons, Inc., Hoboken, New Jersey.
- Phoon, K. K., Santoso, A., and Quek, S. T. 2010. Probabilistic analysis of soil-water characteristic curves. *Journal of Geotechnical and Geoenvironmental Engineering* 136, 445e455.
- Carsel, R. F., and Parrish, R. S. 1988. Developing joint probability distributions of soil water retention characteristics, *Water Resour. Res.* 24 (5), 755–769.
- Silverman, B. W. 1986. Density Estimation for Statistics and Data Analysis. Monographs on Statistics and Applied Probability. Chapman and Hall, London.
- Sheather, S. J., and Jones, M. C. 1991. A reliable data-based bandwidth selection method for kernel density estimation, *J. R. Stat. Soc.*, *Ser. B*, 53, 683–690.
- Sheather, S. J. 2004. Density estimation, Stat. Sci., 19, 588–597.
- van Genuchten, M. T. 1980. A closed-form equation for predicting the hydraulic conductivity of unsaturated soils. *Soil Sci. Soc. Am. J.* 44, 892–898.
- Zhang, X., Mavroulidou, M., and Gunn, M. J. 2017. A study of the water retention curve of limetreated London Clay. *Acta Geotech.* 12 (1), 23–45.
- Zapata, C. E. 1999. *Uncertainty in soil-water characteristic curve and impact on unsaturated shear strength predictions*. Ph.D. Dissertation, Arizona State University, Tempe.